



Application of the HIDRA2 deep-learning model for sea level forecasting along the Estonian coast of the Baltic Sea

Amirhossein Barzandeh¹, Matjaž Ličer^{2,3}, Marko Rus^{2,4}, Matej Kristan⁴, Ilja Maljutenko¹, Jüri Elken¹, Priidik Lagemaa¹, and Rivo Uiboupin¹

¹Department of Marine Systems, Tallinn University of Technology, Tallinn, Estonia

²Slovenian Environment Agency, Ljubljana, Slovenia

³National Institute of Biology, Marine Biology Station, Piran, Slovenia

⁴Faculty of Computer and Information Science, Visual Cognitive Systems Lab, University of Ljubljana, Ljubljana, Slovenia

Correspondence: Amirhossein Barzandeh (amirhossein.barzandeh@taltech.ee)

Received: 26 November 2024 – Discussion started: 29 November 2024

Revised: 8 April 2025 – Accepted: 14 April 2025 – Published: 14 July 2025

Abstract. Sea level predictions, typically derived from 3D hydrodynamic models, are computationally intensive and subject to uncertainties stemming from physical representation and inaccuracies in initial or boundary conditions. As a complementary alternative, data-driven machine learning models provide a computationally efficient solution with comparable accuracy. This study employs the deep-learning model HIDRA2 to forecast hourly sea levels at five coastal stations along the Estonian coastline of the Baltic Sea, evaluating its performance across various forecast lead times. Compared to the regional NEMO_{BAL} and subregional NEMO_{EST} hydrodynamic models, HIDRA2 frequently outperforms both, particularly in terms of overall forecast skill. While HIDRA2 shows limitations in resolving high-frequency sea level variability above $(6\text{ h})^{-1}$, it effectively reproduces energy in lower-frequency bands below $(18\text{ h})^{-1}$. Errors tend to average out over longer time windows encompassing multiple seiche periods, enabling HIDRA2 to surpass the overall performance of the NEMO models. These findings underscore HIDRA2's potential as a robust, efficient, and reliable tool for operational sea level forecasting and coastal management in the eastern Baltic Sea region.

temperatures accelerate its complexity (Bindoff et al., 2007; Cazenave et al., 2014). The increasing frequency and severity of extreme weather events, compounded by rising sea levels due to climate change, present pressing challenges for coastal communities worldwide. Accurate and timely forecasting of sea level is essential for effective disaster preparedness, risk mitigation, and coastal management. However, forecasting sea level variability is inherently complex and requires sophisticated models that account for various drivers and uncertainties. Traditionally, sea level forecasting has been accomplished using hydrodynamic models, but these models are subject to a range of uncertainties induced by errors in atmospheric and open boundary forcing fields, as well as physical flux parameterization (Church et al., 2011; Miles et al., 2014; Khojasteh et al., 2021). Errors in regional sea level prediction can arise from inaccurate initial and boundary conditions, models' approximated descriptions of physical environments (e.g., coupling with waves, atmosphere, ice, and runoff), and the nonlinear nature of planetary dynamics (Carson et al., 2019; Ponte et al., 2019; Hamlington et al., 2020).

Despite these challenges, advancements such as assimilation of observation data in hydrodynamic models have shown promise in improving the accuracy of sea level prediction (Bajo et al., 2019; Barron et al., 2004; Tanajura et al., 2015; Liu and Fu, 2018). However, the computational cost of both ocean modeling and data assimilation adds to the complexity and resource requirements of accurately predicting sea levels (Byrne et al., 2023; Bajo et al., 2023). In this regard, the use

1 Introduction

The importance of sea level variability has grown significantly in the context of climate change as higher global

of data-driven models as a surrogate system can be a promising addition to classic hydrodynamic models for addressing these challenges (Sonnewald et al., 2021). In recent years, machine learning techniques have demonstrated significant potential in enhancing the accuracy and reliability of predictive models in oceanography (Ahmad, 2019; Lou et al., 2023; Jahanmard et al., 2023). Recent studies have highlighted the effectiveness of deep-learning methods in predicting sea level heights across diverse scenarios and basins (Rus et al., 2023; Balogun and Adebisi, 2021; Rajabi-Kiasari et al., 2023; Bahari et al., 2023). However, these studies imply that, unlike hydrodynamic models, deep-learning models require particular structural design and adjustments depending on various objectives, and the specific characteristics of the study area. Additionally, ensemble-based approaches in deep learning, widely employed in practical applications, distinguish themselves from traditional machine learning methods by generating and integrating multiple hypotheses from training data to improve prediction accuracy. This allows for the incorporation of more advanced and diverse algorithms, making it better suited to tackle specific challenges in operational applications (Zhang et al., 2022; Ganaie et al., 2022).

The Baltic Sea, a large, high-latitude, semi-enclosed, and nearly tideless sea located in northern Europe, is a vital marine region characterized by its unique geographical and ecological features. It comprises several sub-basins and is connected to the Atlantic Ocean through the narrow Danish Straits in the southwest. This study specifically focuses on the eastern Baltic Sea, which spans from approximately 21.5–30.5°E longitude and 56.5–61°N latitude. This region encompasses the northeastern Baltic Proper, the Gulf of Finland, and the Gulf of Riga – areas of strategic importance due to the heavy vessel traffic between their populated shores and islands. Understanding sea level changes in the eastern Baltic Sea is therefore vital. Sea level fluctuations affect navigation routes, harbor operations, and maritime safety, making accurate knowledge of these variations essential for stakeholders to manage risks, optimize vessel operations, and ensure efficient trade flows.

Research on sea level variations in the Baltic Sea has revealed a wide range of patterns and trends influenced by numerous environmental factors that vary both spatially and temporally (Andersson, 2002; Ekman, 2009; Hünicke and Zorita, 2016). Historical tide gauge records, used by Jevrejeva et al. (2003) to reconstruct past sea level changes, demonstrate significant interannual and decadal variability attributed to atmospheric pressure fluctuations and shifting wind patterns. Furthermore, the intricate structure of the Estonian coastline, combined with its numerous small islands, poses additional challenges for projecting the impacts of climate change and sea level rise in this region (Johansson et al., 2004; Kont et al., 2008). Although predictions of sea level height on longer temporal scales, such as monthly or weekly, tend to be more accurate due to the smoothing of short-term fluctuations caused by local wind tilt and storm

surges (Samuelsson and Stigebrandt, 1996; Scotto et al., 2009; Elken et al., 2024), short-term sea level changes in the Baltic Sea are heavily influenced by dynamic factors such as wind, precipitation, and the redistribution of water through the Danish Straits (Hünicke et al., 2015). Extreme sea levels on the Baltic coasts, resulting from increasingly frequent storm surges, are influenced by three main factors: the volume of water in the Baltic Sea's basins, which sets the initial sea level; the direction, speed, and duration of tangential wind stresses, whether shoreward or seaward; and the rapid passage of deep low-pressure systems that deform the sea surface, producing seiche-like oscillations that further alter sea levels (Kulikov and Medvedev, 2013; Wolski et al., 2014; Weisse et al., 2021; Wolski and Wiśniewski, 2021; Rutgersson et al., 2022). Seiche oscillations are especially significant in the Baltic Sea due to their prolonged decay over several days. Both the Gulf of Riga and the Gulf of Finland can experience their own seiches with different characteristics (e.g., the 5 h seiche period of the Gulf of Riga, which differs from the recognized seiche period in the Gulf of Finland). These seiches may interact with those from neighboring basins (e.g., the approximately 27 h seiche period of the entire Baltic Sea), leading to complex phase relationships and further complicating sea level predictions (Metzner et al., 2000; Suursaar et al., 2002; Jönsson et al., 2008). This intricate interplay of atmospheric, oceanic, and coastal dynamics makes the prediction of sea level in the Baltic Sea a challenging task.

In response to the increasing demand for accurate and efficient forecasting methods in coastal regions, this study explores the potential of a deep-learning ensemble model. By utilizing deep neural networks, we aim to improve sea level prediction accuracy in the eastern Baltic Sea by applying our approach to a selection of sample stations. The primary focus of this study is to evaluate the effectiveness of a deep-learning ensemble model HIDRA2 (Rus et al., 2023) for sea level forecasting in the study area in multiple lead time windows. A secondary objective is to compare its performance with that of regional and subregional hydrodynamic models currently used for operational purposes in the study area.

2 Data and methods

2.1 Tide gauge data

The hourly sea surface height (SSH) time series were extracted and evaluated as measures of sea level using the available data from five observation stations: Narva-Jõesuu, Pritia, Haapsalu, Pärnu, and Roomassaare (Fig. 1). These stations are situated along the Estonian coast, in the Gulf of Finland and the Gulf of Riga. The datasets were provided by the Estonian Environmental Agency (<https://www.ilmateenistus.ee/>, last access: 4 April 2024) and span the period between 15 June 2010 and 30 April 2024.

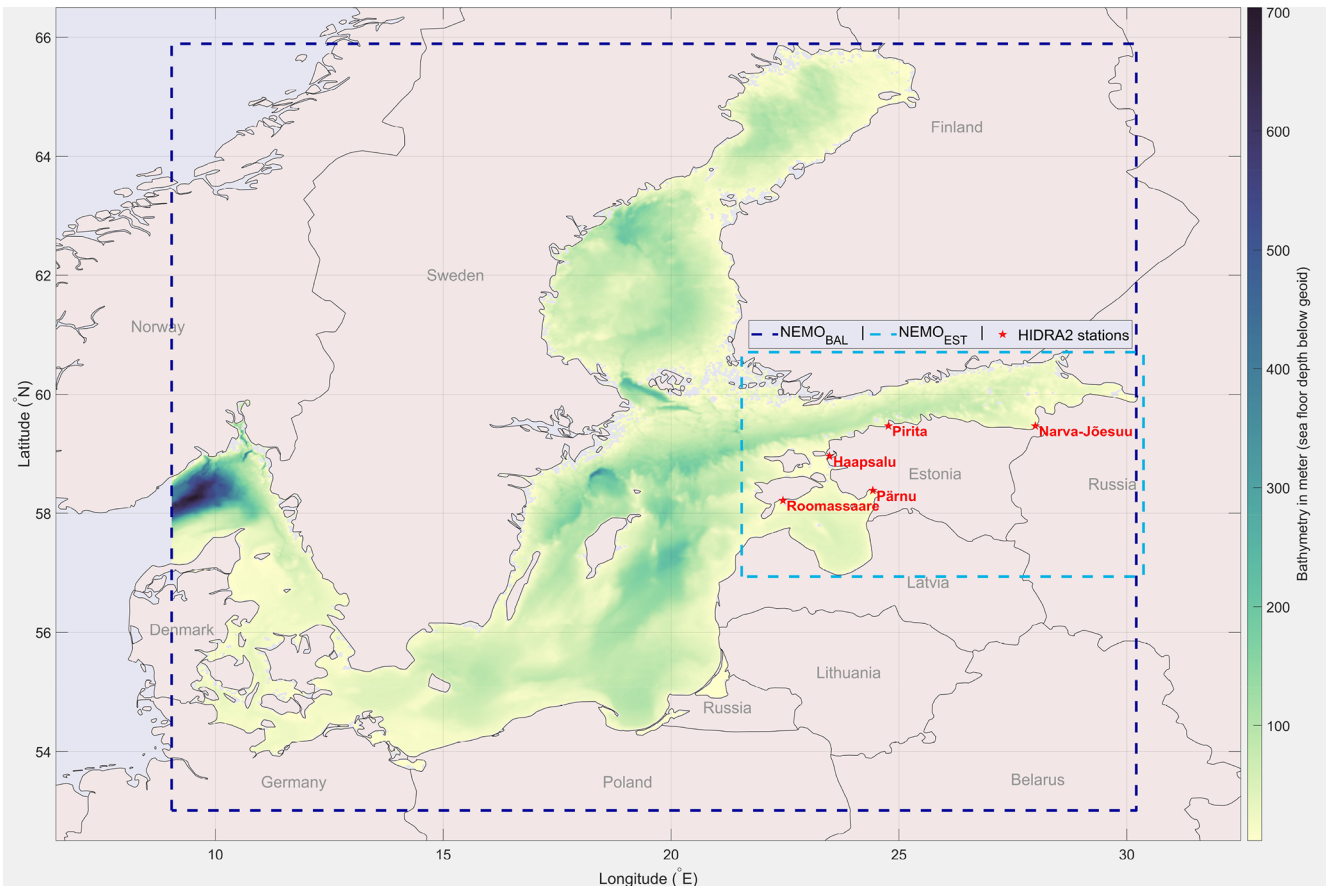


Figure 1. Study area: the domain of each model is illustrated, with red stars indicating the locations of the stations where HIDRA2 has been applied.

2.2 HIDRA2: a deep-learning ensemble sea level forecasting model

HIDRA2 is a state-of-the-art deep-learning model for predicting SSH at specific geographic locations, presented in depth in Rus et al. (2023). The model utilizes historical and predicted atmospheric data, tidal information, and observed SSH measurements to generate precise hourly SSH predictions for a 72 h window. Unlike models that forecast the residual SSH, i.e., the difference between SSH and tide, HIDRA2 predicts the full SSH. The HIDRA2 architecture, illustrated in Fig. 2, incorporates specialized encoders for processing both atmospheric data and sea level inputs. The atmospheric encoder processes wind and pressure sequences, subsequently merging them into a unified feature representation. The SSH encoder processes historical SSH data. In the fusion-regression block, all extracted features with the preceding 72 h raw SSH data are fused and regressed into final SSH forecasts. These encoders consist of a series of convolution layers, activation functions, dropout layers, and skip connections, forming a robust and deep neural network. Details of the encoding architecture are presented in Rus et al.

(2023). The specific difference in this study for the Baltic Sea application is that, unlike in Rus et al. (2023), HIDRA2 was trained on the full SSH data rather than on separate tidal and SSH signals. This decision was made because tides in the Baltic are very weak, and the explicit inclusion of tides as a separate input signal did not improve forecasting performance. Consequently, we removed the tidal encoder block and fused only the atmospheric and SSH features, augmented by the raw SSH measurements, to produce the final set of 72 h SSH predictions.

For the training of HIDRA2, we utilized atmospheric data fields from the European Centre for Medium-Range Weather Forecasts (ECMWF) Ensemble Prediction System (Leutbecher and Palmer, 2007). For all locations, we used 10 m winds and mean sea level air pressure from a single atmospheric ensemble member, covering a longitudinal range from 16.25 to 28.5° E and a latitudinal range from 54.25 to 64° N. This selection was guided by iterative testing aimed at minimizing forecast errors. The original meteorological data, with a domain size of 40 × 50, were subsampled to a 9 × 12 grid using bilinear interpolation to match HIDRA2's required input size. This transformation reduced dimension-

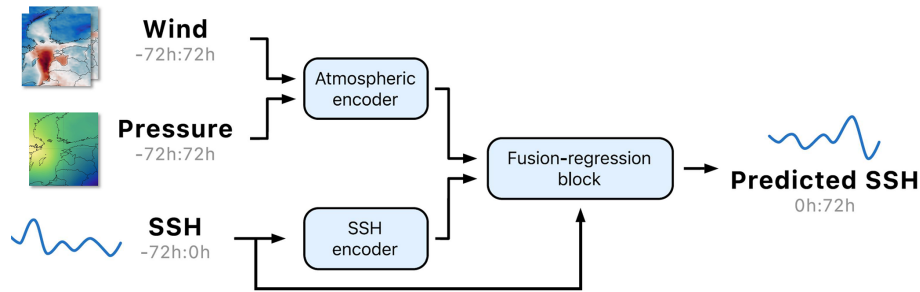


Figure 2. HIDRA2 architecture. The structure of the building blocks is inherited from HIDRA2 and explained in detail in Rus et al. (2023).

ality while preserving key spatial patterns, facilitating more efficient model training. We also conducted experiments using the full-resolution atmospheric fields. These trials involved necessary adjustments and fine-tuning of the model. However, we found that the resulting performance metrics were comparable to those achieved with the subsampled data, showing no significant improvement despite the increased computational demand. Given the similar performance and the considerable advantage in computational efficiency, we retained the subsampled approach for the results presented. The training data for SSH at the coastal stations were obtained from the Estonian Environmental Agency as mentioned in Sect. 2.1. However, the SSH data used for training consisted of hourly observations from 2010 to 2019 at all locations, while the period from April 2023 to April 2024 was utilized for testing the model and performing the analyses presented in this study. Following the methodology outlined by Rus et al. (2023), we trained a separate HIDRA2 model for each of the five geographic locations depicted in Fig. 1.

2.3 NEMO_{BAL}: a forecast product based on a regional hydrodynamic modeling

We extracted the Baltic Sea Physics Analysis and Forecast datasets (BALTIC-SEA_ANALYSIS_FORECAST_PHY_003_006, 2024) from the Copernicus Marine Service for each station in the study area over the study period. This forecast product is based on the NEMO 4.0 ocean engine, specifically configured for the North Sea and Baltic Sea as Nemo-Nordic 2.0 (Madec et al., 2017; Kärnä et al., 2021), and has been implemented and validated by the Baltic Monitoring and Forecasting Centre (BALMFC) to address the needs of the Baltic Sea region. For brevity, we refer to it as NEMO_{BAL} in this study. The product offers a spatial resolution of 1 nautical mile (nmi) and is updated twice daily, providing new 6 d forecasts. Consequently, the dataset records available from Copernicus include only 12 h forecasts. The detailed validation report is given in Jandt-Scheelke et al. (2023).

2.4 NEMO_{EST}: a subregional hydrodynamic forecasting model

NEMO-EST05 is the Estonian adaptation of the Baltic Sea regional configuration Nemo-Nordic 2.0 with enhanced horizontal and vertical resolution, tailored for national operational purposes (hereafter referred to as NEMO_{EST}). Detailed specifications of this model are provided in Maljutenko et al. (2022), and an example of its utilization is presented in Pärt et al. (2023). NEMO_{EST} uses the same NEMO 4.0 ocean engine with a horizontal resolution of 0.5 nmi spanning from 21.5 to 30.5° E and from 56.5 to 60.5° N. The meteorological forcing for the model system is obtained from the ECMWF 24 h integrated forecasting system (Owens and Hewson, 2018). Boundary conditions for salinity, temperature, and sea levels are derived from the same NEMO_{BAL}, following the methodology outlined by Elken et al. (2021). Model initialization in the October 2022 is from the NEMO_{BAL}. It can be inferred that NEMO_{EST} serves as a downscaled version of NEMO_{BAL}. Therefore, using both models in the present study also provides implicit insights into how the spatial resolution of hydrodynamic models, as well as their domain extent, affects SSH forecasting.

2.5 Forecasting and evaluation framework

HIDRA2 and NEMO_{EST} provide SSH forecasts for the next 72 h, segmented into three 24 h intervals: 0 to 24 h (24), 24 to 48 h (48), and 48 to 72 h (72), with daily updates. This segmentation allows for the evaluation of model performance at different lead times up to 72 h. Regardless of the training time window used for the deep-learning model, the testing period of all models in the present study spans 1 year, from 1 April 2023 to 31 March 2024 (in total, 8784 h time instances). This period aligns with the initiation of archiving 72 h SSH fields in NEMO_{EST} from its daily forecast cycles. For comparison, NEMO_{BAL} was also considered as the publicly available SSH forecast for the study area. To ensure a fair comparison and address potential bias from the reference sea level in the hydrodynamic models (NEMO_{BAL} and NEMO_{EST}), the outputs were adjusted by removing their mean value over the study period and then adding the mean

observed SSH at each station. This adjustment to the datums of the local observation system ensures that the outputs of the hydrodynamic models are comparable to the observed values, whereas HIDRA2, as a data-driven model, is not subject to this type of reference sea level bias. Additionally, HIDRA2, as an ensemble forecasting system, produces 50 distinct forecast ensembles at each time point. In the analysis, unless specifically examining individual ensembles, the HIDRA2 forecasts are represented by the average of all 50 ensembles for each time instance and station. Using the mean of all ensembles as the final forecast is appropriate because the ensembles represent probabilities without any inherent priority in real-world occurrences.

Furthermore, the performance of the forecasts is also separately evaluated during extreme negative and positive observed SSH events. Extreme negative SSH values are defined as those falling below the 5th percentile of observed SSH at each station during the study period, while extreme positive values are those exceeding the 95th percentile (Cannaby et al., 2016; Mentaschi et al., 2023).

2.6 Validation metrics

The validations and comparisons in the present study include the Pearson correlation coefficient (correlation) and the root mean square deviation (RMSD). Each is defined as follows.

RMSD is given by Eq. (1):

$$\text{RMSD} = \left(\frac{1}{n} \sum_{i=1}^n (o_i - m_i)^2 \right)^{1/2}, \quad (1)$$

where n represents the total number of observations, and o_i and m_i are the observed and modeled sea level values, respectively.

Correlation is defined by Eq. (2):

$$\text{correlation} = \frac{1}{\sigma_m \sigma_o} \sum_{i=1}^n (m_i - \bar{m})(o_i - \bar{o}), \quad (2)$$

where \bar{m} and \bar{o} are the mean values of the modeled and observed datasets, respectively.

The standard deviations of the modeled and observed datasets, σ_m and σ_o , are calculated as shown in Eq. (3):

$$\sigma_m = \left(\sum_{i=1}^n (m_i - \bar{m})^2 \right)^{1/2}, \quad \sigma_o = \left(\sum_{j=1}^n (o_j - \bar{o})^2 \right)^{1/2}. \quad (3)$$

The validation metrics for each station are calculated using referenced to the SSH observation data from April 2023 to April 2024.

3 Results

3.1 Comparison of models' overall performance

Table 1 presents the RMSD values for the forecasts across all tide gauge stations relevant to availability of the model outputs in the present study. At 24 h lead time, the HIDRA2 ensemble mean consistently achieves the lowest RMSD at each station, outperforming even NEMO_{BAL}, which inherently includes 12 h lead-time forecasting. HIDRA2 with a 72 h lead time also demonstrates performance comparable to NEMO_{BAL} at Roomassaare and Pärnu. Remarkably, HIDRA2 exhibits substantially lower RMSD at other stations, even with extended forecast lead times.

Several studies such as Campos-Caba et al. (2024) and Mentaschi et al. (2013) have highlighted limitations in using the RMSD as a standalone performance metric, particularly due to the double-penalty effect. This occurs when temporal mismatches between modeled and observed seiches lead to models being penalized twice: once for predicting a peak that did not occur and again for failing to predict one that did. As a result, RMSD may not fully capture the quality of model predictions. To address this, RMSD should be interpreted alongside complementary performance metrics. For instance, Campos-Caba et al. (2024) propose evaluating the mean absolute deviation, adjusted across percentiles by the corresponding mean absolute deviation of each percentile from the 0th to the 100th percentile in 1 % steps.

We therefore recommend that Table 1 and the RMSD values be considered in conjunction with the model error across all sea level bins (Fig. 3) and further contextualized through spectral analysis of model and observed time series.

Figure 3 illustrates the forecast RMSD by sea level bin (0.05 m) for all models at different lead times. HIDRA2 with a 24 h lead time generally outperformed the other models, achieving the lowest RMSD across most of the sea level distribution, i.e., at all sea level percentile bins p . However, in the tails of the distribution (SSH > 1.00 m or SSH < -0.40 m), RMSDs increased for all models. At extreme sea levels, HIDRA2 and NEMO_{BAL} demonstrated similarly robust performance, albeit with differences depending on lead time. HIDRA2 showed solid performance at the 24 h lead time but struggled in the distribution tails at the 72 h lead time.

Figure 3 highlights that HIDRA2's advantage over NEMO_{BAL} primarily stems from its superior performance in the bulk of the distribution and at extreme low SSH values. This distinction is particularly evident at the Haapsalu station.

Additionally, the accuracy of each model, integrated across all study stations, is compared using Taylor diagrams (Taylor, 2001) in Fig. 4a. The 5th and 95th percentile thresholds for each station are provided in Table 2. HIDRA2 consistently outperformed both hydrodynamic models, showing the lowest RMSD and highest correlation coefficients across

Table 1. RMSD metrics of the three forecast models for the April 2023 to April 2024 period. Results are separated by the forecast lead times (12, 24, and 72 h). Lowest RMSDs are in bold.

Station	12 h RMSD (m)		24 h RMSD (m)		72 h RMSD (m)	
	NEMO _{BAL}	NEMO _{EST}	HIDRA2	NEMO _{EST}	HIDRA2	NEMO _{EST}
Roomassaare	0.051	0.058	0.033	0.063	0.051	0.063
Pärnu	0.074	0.074	0.051	0.083	0.074	0.083
Haapsalu	0.099	0.090	0.040	0.095	0.063	0.095
Piritia	0.056	0.059	0.039	0.067	0.054	0.067
Narva-Jõesuu	0.079	0.074	0.039	0.090	0.075	0.090

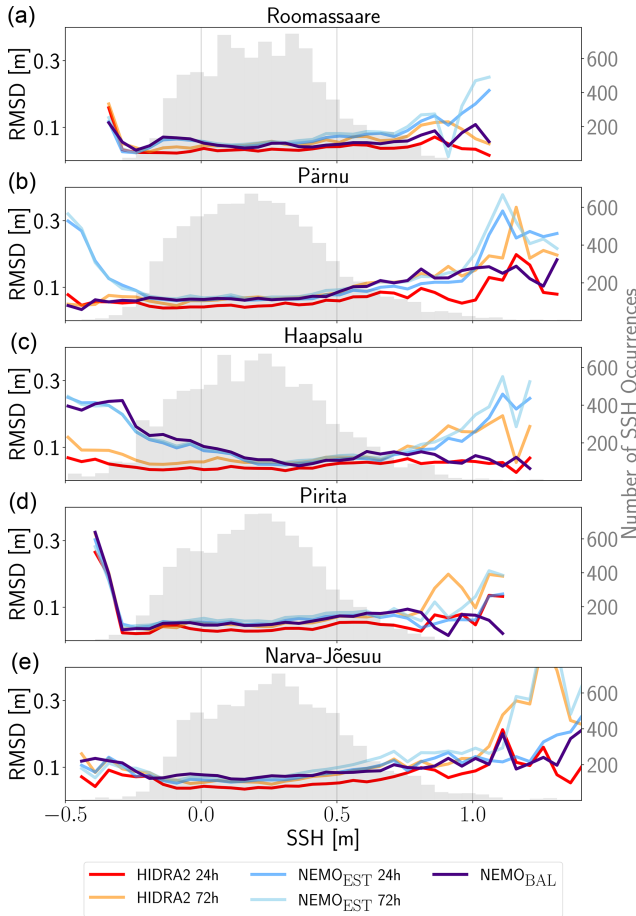


Figure 3. RMSD of all forecast models (colored lines; see legend at the bottom) at different sea level values. Grey histogram in the back (right axis) shows the distribution of occurrences of a given sea level bin.

most observed SSH ranges. Although HIDRA2’s accuracy declines for extreme SSH values, particularly at extended lead times, it still surpasses both regional and subregional hydrodynamic models, except at 72 h lead time. Among the hydrodynamic models, the regional model NEMO_{BAL} performs best during extreme SSH events, while the subregional model NEMO_{EST} performs better under non-extreme high

Table 2. Thresholds for SSH used to identify extreme positive and negative storm surges at each station.

Stations	SSH _{5th} percentile	SSH _{95th} percentile
Roomassaare	−0.11	0.67
Pärnu	−0.16	0.71
Haapsalu	−0.21	0.66
Piritia	−0.15	0.60
Narva-Jõesuu	−0.10	0.76

SSH conditions but struggles to accurately predict extreme SSH values.

We perform an independent analysis of the predictive accuracy across the 50 members of the HIDRA2 ensemble, evaluating each member’s forecasts of SSH values. As expected, increasing the lead time of forecasts results in reduced accuracy of each predicted ensemble member. Both the correlation coefficient and RMSD vary across different lead times, and the spread of ensemble predicted values increases with longer lead times. This spread is especially pronounced during extreme observed SSH values. For negative extreme SSH events, correlation is lower with a lower RMSD, while for positive extreme SSH events, correlation is higher but with a higher RMSD (Fig. 5).

3.2 Specific challenges in model performance

Overall, HIDRA2 forecasts with a 24 h lead time consistently outperformed throughout the study period at all stations, as detailed in Table 1 (an overview of the reliable forecast capabilities of HIDRA2 is also provided in the Supplement). However, a closer examination, as shown in Fig. 6, reveals that HIDRA2 predictions are overly smoothed, lacking the ability to fully capture high-frequency variability (with periods below 6 h). In contrast, NEMO_{BAL} demonstrates better performance in this energy band. Figure 6 highlights model forecasts with a 24 h lead time during October 2023, a period marked by a series of extreme sea level events.

A visual comparison of model predictions in Fig. 6 between 5 and 9 October 2023 is highly indicative. (To further aid recognition, this specific time window is highlighted by an orange box in Fig. 6.) Sea levels in Pärnu indicate the

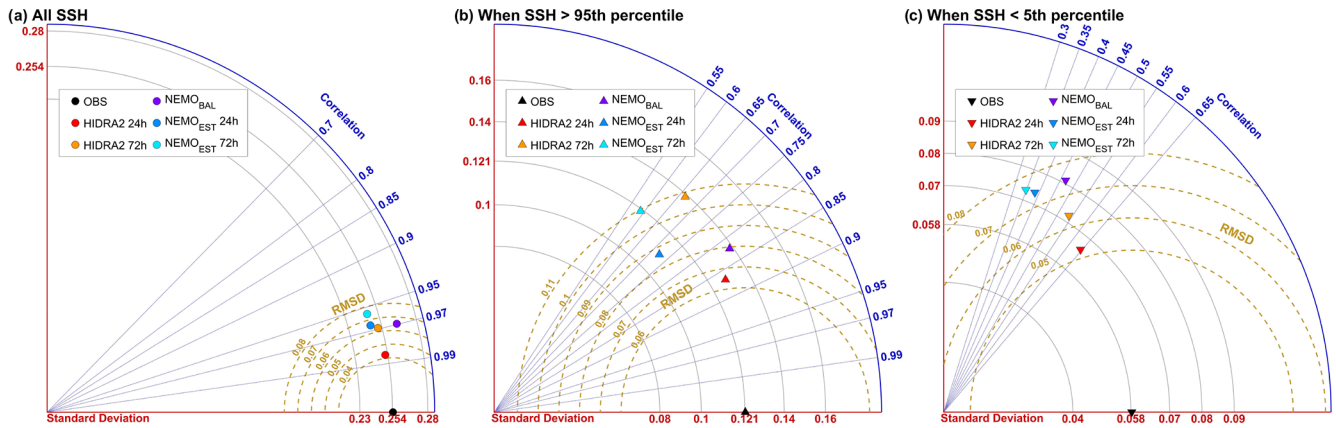


Figure 4. Taylor diagrams comparing forecasts: (a) all hourly time instances, (b) positive extreme SSH, and (c) negative extreme SSH.

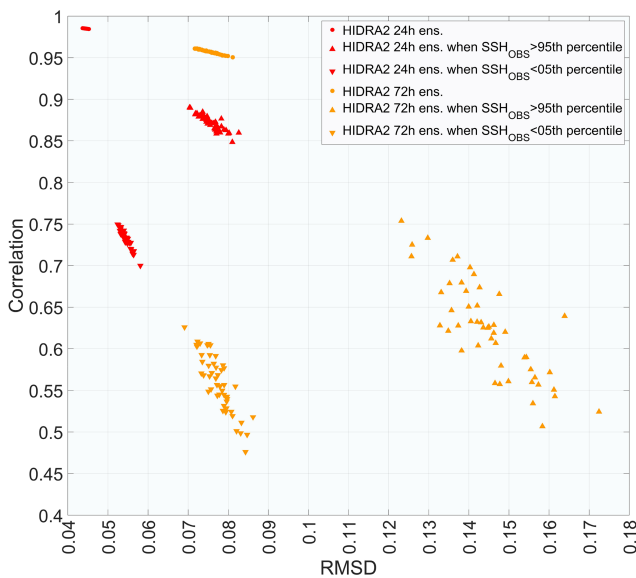


Figure 5. Performance of individual HIDRA2 ensemble members at 24 and 72 h lead times and a further assessment under the conditions of the positive and negative extreme observed SSH.

presence of the fundamental seiche with a period around 5 h. NEMO_{BAL} reproduces this excitation very clearly, while it is practically completely absent from the HIDRA2 forecast. A similar scenario occurs on 13 October – NEMO_{BAL} exhibits high-frequency variability, whereas the HIDRA2 ensemble mean is completely smooth. This smoothing effect could potentially result from averaging over the ensemble members, where oscillations present in individual members cancel each other out. This is however not the case. None of the ensemble members exhibit enough excitations in the Pärnu seiche energy band (not shown).

The limitations of HIDRA2 during seiche excitations can be evaluated by applying a band-pass filter to the sea level signal in the Pärnu seiche energy band for the period of ex-

cited seiches between 5 and 9 October 2023. We use a sixth-order Butterworth filter with a sample rate of 1 h and low and high cutoff frequencies of $(3\text{h})^{-1}$ and $(8\text{h})^{-1}$, respectively (Fig. 7). The filtered observations in Fig. 7 clearly show the excitation of the seiches starting on 3 October, which is also captured by NEMO_{BAL}. In contrast, the HIDRA2 ensemble mean is overly smooth, rendering it less capable of reproducing sea level variability within the seiche frequency band. However, it adheres more closely to the overall observations than NEMO_{BAL}. HIDRA2’s limited accuracy during seiche excitations leads to deviations from instantaneous sea level values, increasing the short-term errors. However, over periods of several days, HIDRA2 exhibits minimal bias. This indicates that while individual hourly predictions may show higher error, HIDRA2’s forecasts do not consistently over- or underestimate SSH over longer time spans, resulting in minimal systematic bias.

This experiment also demonstrates the value of the ensemble prediction. While separate members of the HIDRA2 ensemble (and consequently their ensemble mean as well) are not capable of capturing the high-frequency variability of the seiche (not shown), this limitation is partly compensated by the ensemble spread, which to some extent envelops the actual amplitude of the seiches. Therefore, the sea levels during the seiche will often still be within the ensemble envelope, although the seiche itself is poorly reproduced in each individual ensemble member. This ensemble approach in HIDRA2 is especially useful for addressing the challenges of triggering events and managing uncertainty in sea level forecasts. Triggering events often involve abrupt and transient atmospheric or oceanic changes, like storms or pressure systems, which lead to rapid sea level shifts. While HIDRA2’s ensemble mean may not directly capture these fluctuations, the ensemble spread creates a “buffer” around the observed values. This means that during trigger events, even if individual ensemble members miss exact timings or magnitudes, the ensemble as a whole may still envelop the observed extremes, providing a probabilistic signal of potential risks.

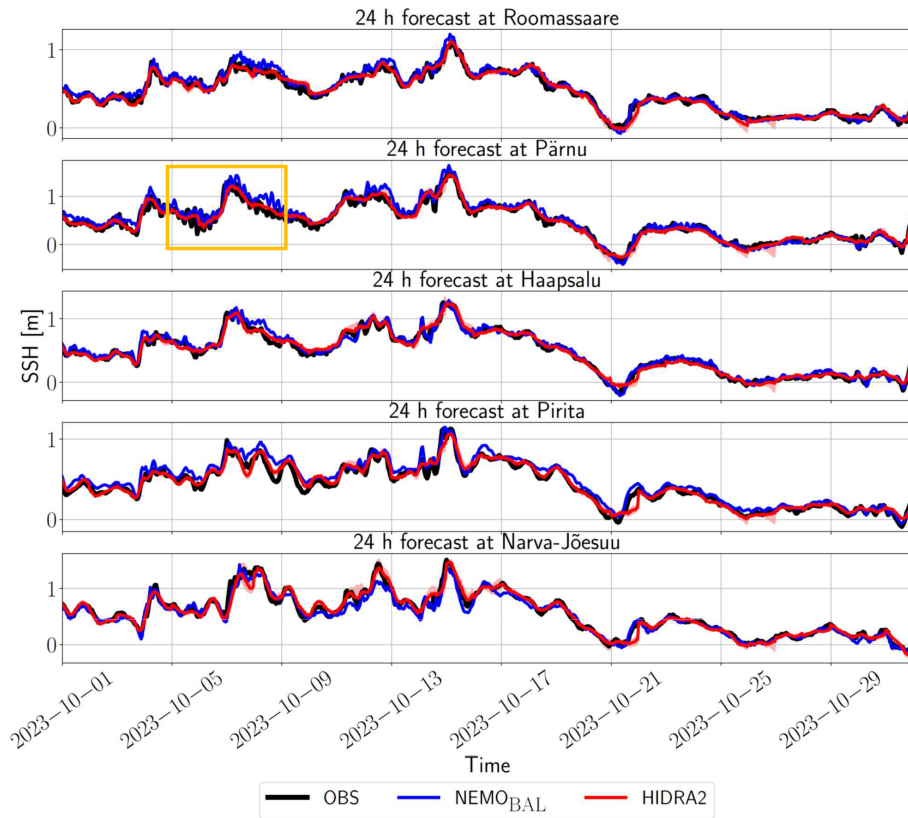


Figure 6. Observed SSH (black line) vs. NEMO_{BAL} (blue line) and HIDRA2 ensemble mean (red line) forecasts with a 24 h lead time at various stations during October 2023.

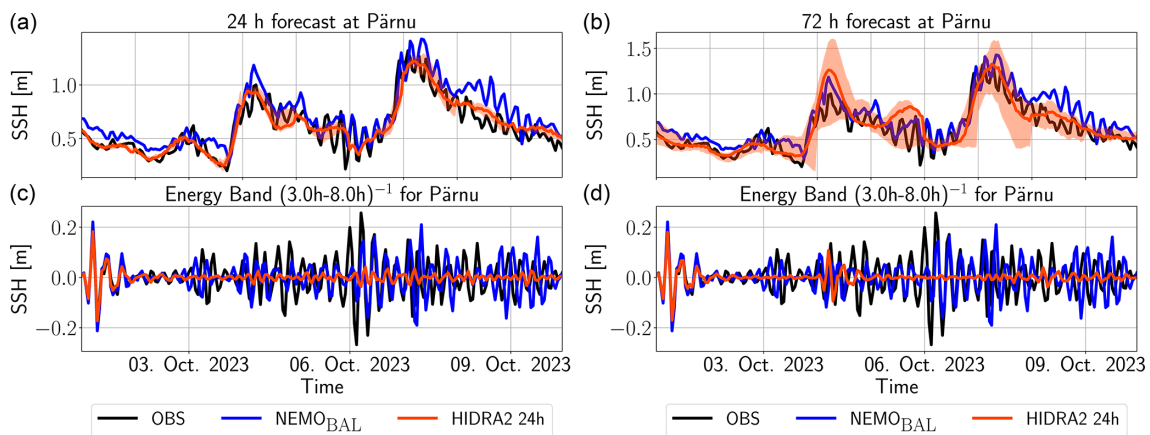


Figure 7. (a, b) Sea levels in Pärnu during the seiche between 5–9 October 2023 for 24 h (a, c) and 72 h (b, d) lead times. Orange area denotes the limits of the HIDRA2 ensemble envelope. (c, d) Bandpass-filtered sea levels in the frequency band $(3\text{h})^{-1}$ – $(8\text{h})^{-1}$ during the same period and for the same lead times. Note the different vertical scales in both plots.

To quantify NEMO_{BAL}, as well as HIDRA2 behavior in different spectral bands, we computed power spectral densities (PSDs) for observations and model forecasts for each of the stations, as shown in Fig. 8. The PSD was calculated by normalizing the squared magnitude of the fast Fourier transform coefficients at each frequency, followed by an inver-

sion of frequencies to periods. This allowed us to identify dominant seiche periods and the (ir)relevance of tidal forcing (peaks around 12 and 24 h). In Pärnu, for example, the fundamental seiche peak close to 6 h period is quite prominent, while the semi-diurnal 12 h peak does not stand out in its energy band, indicating that semi-diurnal tides are not driving

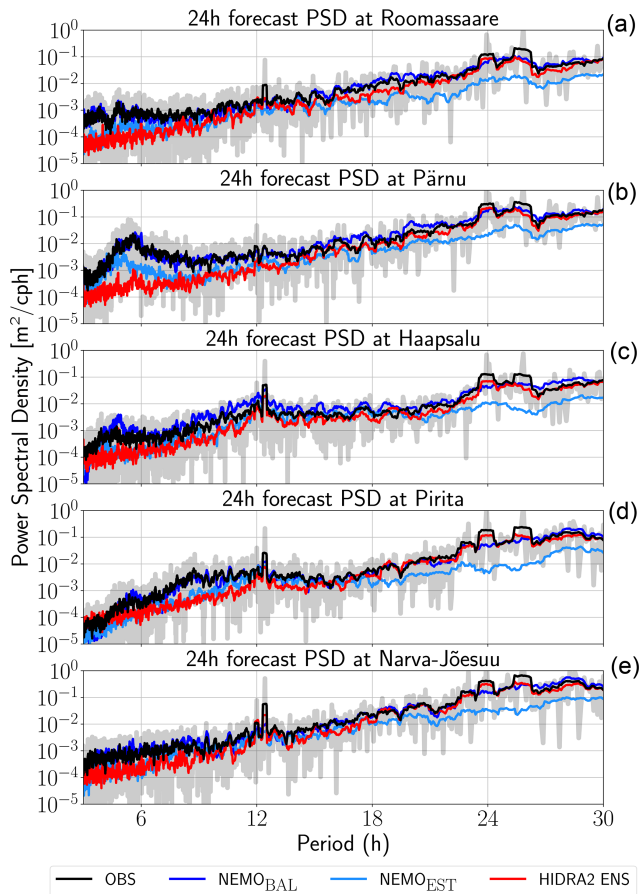


Figure 8. Power spectral densities [$\text{m}^2\text{cph}^{-1}$] of sea levels from different sources (colored lines; see legend at the bottom) at each station (rows). Grey lines in the back denote raw spectra, while black lines denote their 6 h moving average; cph indicates cycles per hour.

the dynamics at this station. At other stations, for example, semi-diurnal tides are a bit more pronounced.

The spectra reveal that HIDRA2 faces challenges in fully capturing seiche dynamics and tends to underestimate energy density in the subinertial energy band (at the latitude of Pärnu, this corresponds to periods below 13 h or rather frequencies above $(13\text{ h})^{-1}$) – in this band NEMO_{BAL} accurately reproduces the observed amount of energy. HIDRA2 spectra are however the closest to observations spectra in the band with periods above 18 h. Especially at diurnal tide band HIDRA2 shows slightly better performance than NEMO_{BAL}, while both HIDRA2 and NEMO_{BAL} outperform NEMO_{EST}. This corresponds to the solid overall performance of HIDRA2 and its poor reproduction of high-frequency variability. NEMO_{EST} on the other hand lacks almost an order of magnitude of energy in the energy band with periods above 18 h but indicates a decent reproduction of the Pärnu seiche.

4 Discussion

Validation metrics, such as RMSD and correlation coefficient, presented in this study underscore HIDRA2's competitive performance compared to other sea level forecasting methods, as demonstrated in other studies (e.g., Ishida et al., 2020; Shahabi and Tahvildari, 2024; Dong et al., 2024). Despite the influence of various regional factors on short-term SSH forecasts, the primary distinction between HIDRA2 and methods used in previous studies is the utilization of a deep-learning “ensemble” approach. Thus, the effectiveness of HIDRA2 in this case study underscores the importance of incorporating diverse ensembles to account for varying short-term atmospheric conditions and climate scenarios (Gröger et al., 2019; Hieronymus and Hieronymus, 2023). For operational applications, particularly in decision-making and initiating specific response phases, HIDRA2 can be more effective when the triggering limits are set to the maximum and minimum ensemble values, as these represent the most probable scenarios. Although the probability of reaching the maximum or minimum ensemble values in typical cases is around 2% – given the 50 ensembles used in this study – the ensemble spread, which almost always encompasses the absolute SSH values, suggests that HIDRA2 is a more reliable tool for operational forecasting and triggering. This reliability is especially notable when compared to other forecasting systems that do not provide ensemble predictions. Future studies could further explore optimizing this ensemble range. In the present study, it has been shown that the spread of ensemble-predicted values increases with longer lead times, with this spread becoming particularly pronounced during extreme observed SSH values. When considering a separate evaluation of negative and positive extreme SSH events, the results show that for negative extreme SSH events, the correlation is lower with a narrower RMSD, while for positive extremes, the correlation is higher but accompanied by a wider RMSD. Here, the significance of comparing RMSDs may be less relevant, as higher RMSD values can be acceptable when target values are higher. But, in general, the lower correlation during negative SSH extremes suggests that while the model captures some general trends or patterns, it does not align well with the exact fluctuations or magnitudes of observed values. From a data-driven modeling perspective, this may be explained by data imbalance: negative extreme events are rarer than positive extremes in the study area (Conte and Lionello, 2013; Jensen et al., 2022), providing HIDRA2 with fewer examples of negative events during training. Consequently, HIDRA2 may perform better for positive extreme events, having learned from their relatively higher frequency. This observation demonstrates the model's enhanced capability to capture more common extreme event types. This stems from HIDRA2's data-driven foundation, which allows it to effectively learn patterns from densely populated regions of the training distribution. In contrast, hydrodynamic models, while grounded in first-principles physics, are generally

less responsive to data frequency and often lack flexibility in probabilistic forecasting. To further improve HIDRA2's performance across the full range of sea level conditions – particularly in data-sparse regimes – future developments could explore the integration of physics-informed neural networks (Raissi et al., 2019; Zhu et al., 2025). By incorporating physical constraints, such as conservation laws or shallow water dynamics, into the learning process, such approaches can mitigate the effects of limited data availability while guiding the model toward physically consistent behavior, even under rare or extreme scenarios. Looking ahead, combining physics-informed strategies with ensemble-based deep learning may provide a more robust and generalizable framework for sea level forecasting, supporting both routine operations and high-impact coastal applications.

5 Conclusions

This study evaluates an implementation of HIDRA2, a deep-learning sea level model, alongside two numerical models: NEMO_{EST}, a subregional hydrodynamic model with a spatial resolution of 0.5 nmi, and NEMO_{BAL}, a regional hydrodynamic model with a spatial resolution of 1 nmi and 12 h lead time. In summary, based on the averaged correlation coefficient and RMSD across the study period between modeled and observed SSH, the results indicate that HIDRA2 generally outperforms the hydrodynamic models.

While accuracy decreases in predicting extreme sea level events, the observed values generally fall within the predicted ensemble spread of HIDRA2, highlighting its overall reliability. However, some open issues remain. HIDRA2 did not perfectly reproduce seiches in Pärnu Bay and in general lacks energy in the subinertial band with periods below 13 h. Reproduction of sea level dynamics in this band is something that will have to be addressed in further work. This can be partly offset by an ensemble spread, but the spread with 24 h lead time is underestimated, while the spread for 72 h seems overestimated, as can be seen from Fig. 7.

These issues might be addressed by further implementations of a very recent version of HIDRA (Rus et al., 2025), which is capable of performing multipoint predictions. Preliminary investigations (not shown) however indicate that high-frequency sea level variability is a very difficult task for classical models and for deep networks. As far as deep networks are concerned, it is currently unclear whether poor reproduction of this spectral band is an issue of architecture or of insufficient training data. In any case this task should have a high priority of research due to its ever-growing relevance for business and safety under most climate change sea level rise scenarios.

Code availability. The persistent version of the GitHub repository containing HIDRA2 code is available at <https://doi.org/10.5281/zenodo.7307365> (Rus et al., 2022).

Data availability. SSH observation data for each studied station are available from the Estonian Environmental Agency (<https://keskkonnaportaal.ee/et/avaandmed/hydroloogilise-seire-andmestik>, Estonian Environment Agency, 2024). Atmospheric inputs used for training and running the models in this study can be obtained from the ECMWF (<https://www.ecmwf.int/en/forecasts/datasets>, ECMWF, 2024). Baltic Sea Physics Analysis and Forecast datasets (referred to as NEMO_{BAL} in this study) are accessible through the EU Copernicus Marine Service under the dataset identifier BALTICSEA_ANALYSISFORECAST_PHY_003_006 (<https://doi.org/10.48670/moi-00010>, CMEMS, 2024).

Supplement. The supplement related to this article is available online at <https://doi.org/10.5194/os-21-1315-2025-supplement>.

Author contributions. All authors contributed to discussions and editing of the paper. AB conducted model runs and data extractions for the study area, pre- and post-processed the outputs, analyzed and prepared the final results, and drafted the original manuscript. MR and MK prepared and trained the HIDRA2 model for the case study. ML performed spectral analyses and wrote parts of the manuscript. AB and ML plotted the figures. ML, IM, and RU contributed to the design and conceptualization of the study and provided advisory input on the methodology. IM, JE, and PL conducted the NEMO_{EST} runs and prepared and preprocessed the related data.

Competing interests. The contact author has declared that none of the authors has any competing interests.

Disclaimer. Publisher's note: Copernicus Publications remains neutral with regard to jurisdictional claims made in the text, published maps, institutional affiliations, or any other geographical representation in this paper. While Copernicus Publications makes every effort to include appropriate place names, the final responsibility lies with the authors.

Special issue statement. This article is part of the special issue "Special issue on ocean extremes (55th International Liège Colloquium)". It is not associated with a conference.

Acknowledgements. This research was funded by the EU through agreement DE_330_MF between ECMWF and Météo-France. Additional support was provided by the EU and the Estonian Research Council under project TEM-TA38 (Digital Twin of Marine Renewable Energy). Furthermore, this work received funding through the AdapEST project ("Implementation of national climate

change adaptation activities in Estonia, VEU23019”), supported by the European Climate, Infrastructure and Environment Executive Agency (CINEA) via the LIFE program. Matjaž Ličer acknowledges the financial support from the Slovenian Research and Innovation Agency ARIS (contract no. P1-0237).

Financial support. This research has been supported by the European Centre for Medium-Range Weather Forecasts (grant no. DE_330_MF), the Estonian Research Council (grant no. TEM-TA38), the European Commission (grant no. VEU23019), and the Slovenian Research and Innovation Agency ARIS (grant no. P1-0237).

Review statement. This paper was edited by Antonio Ricchi and reviewed by Giovanni Liguori and one anonymous referee.

References

- Ahmad, H.: Machine learning applications in oceanography, *Aquatic Research*, 2, 161–169, <https://doi.org/10.3153/AR19014>, 2019.
- Andersson, H.: Influence of long-term regional and large-scale atmospheric circulation on the Baltic sea level, *Tellus A*, 54, 76–88, <https://doi.org/10.3402/tellusa.v54i1.12125>, 2002.
- Bahari, N. A. A. B. S., Ahmed, A. N., Chong, K. L., Lai, V., Huang, Y. F., Koo, C. H., Ng, J. L., and El-Shafie, A.: Predicting sea level rise using artificial intelligence: a review, *Arch. Comput. Method. E.*, 30, 4045–4062, <https://doi.org/10.1007/s11831-023-09934-9>, 2023.
- Bajo, M., Medugorac, I., Umgiesser, G., and Orlić, M.: Storm surge and seiche modelling in the Adriatic Sea and the impact of data assimilation, *Q. J. Roy. Meteor. Soc.*, 145, 2070–2084, <https://doi.org/10.1002/qj.3544>, 2019.
- Bajo, M., Ferrarin, C., Umgiesser, G., Bonometto, A., and Coraci, E.: Modelling the barotropic sea level in the Mediterranean Sea using data assimilation, *Ocean Sci.*, 19, 559–579, <https://doi.org/10.5194/os-19-559-2023>, 2023.
- Balogun, A.-L. and Adebisi, N.: Sea level prediction using ARIMA, SVR and LSTM neural network: assessing the impact of ensemble Ocean-Atmospheric processes on models’ accuracy, *Geomat. Nat. Haz. Risk*, 12, 653–674, <https://doi.org/10.1080/19475705.2021.1887372>, 2021.
- BALTICSEA_ANALYSIS_FORECAST_PHY_003_006: E.U. Copernicus Marine Service Information (CMEMS), Marine Data Store (MDS), Copernicus Marine Service [code], <https://doi.org/10.48670/moi-00010>, 2024.
- Barron, C., Birol Kara, A., Hurlburt, H., Rowley, C., and Smedstad, L.: Sea surface height predictions from the global Navy Coastal Ocean Model during 1998–2001, *J. Atmos. Ocean. Tech.*, 21, 1876–1893, <https://doi.org/10.1175/JTECH-1680.1>, 2004.
- Bindoff, N., Willebrand, J., Artale, V., Cazenave, A., Gregory, J., Gulev, S., Hanawa, K., Le Quere, C., Levitus, S., and Nojiri, Y.: Observations: oceanic climate change and sea level, <https://nora.nerc.ac.uk/id/eprint/15400> (last access: 13 July 2025), 2007.
- Byrne, D., Horsburgh, K., and Williams, J.: Variational data assimilation of sea surface height into a regional storm surge model: benefits and limitations, *J. Oper. Oceanogr.*, 16, 1–14, <https://doi.org/10.1080/1755876X.2021.1884405>, 2023.
- Campos-Caba, R., Alessandri, J., Camus, P., Mazzino, A., Ferrari, F., Federico, I., Vousedoukas, M., Tondello, M., and Mentaschi, L.: Assessing storm surge model performance: what error indicators can measure the model’s skill?, *Ocean Sci.*, 20, 1513–1526, <https://doi.org/10.5194/os-20-1513-2024>, 2024.
- Cannaby, H., Palmer, M. D., Howard, T., Bricheno, L., Calvert, D., Krijnen, J., Wood, R., Tinker, J., Bunney, C., Harle, J., Saulter, A., O’Neill, C., Bellingham, C., and Lowe, J.: Projected sea level rise and changes in extreme storm surge and wave events during the 21st century in the region of Singapore, *Ocean Sci.*, 12, 613–632, <https://doi.org/10.5194/os-12-613-2016>, 2016.
- Carson, M., Lyu, K., Richter, K., Becker, M., Domingues, C. M., Han, W., and Zanna, L.: Climate model uncertainty and trend detection in regional sea level projections: a review, *Surv. Geophys.*, 40, 1631–1653, <https://doi.org/10.1007/s10712-019-09559-3>, 2019.
- Cazenave, A., Dieng, H.-B., Meyssignac, B., Von Schuckmann, K., Decharme, B., and Berthier, E.: The rate of sea-level rise, *Nat. Clim. Chang.*, 4, 358–361, <https://doi.org/10.1038/nclimate2159>, 2014.
- Church, J., Gregory, J., White, N., Platten, S., and Mitrovica, J.: Understanding and projecting sea level change, *Oceanography*, 24, 130–143, <https://doi.org/10.5670/oceanog.2011.33>, 2011.
- CMEMS – EU Copernicus Marine Service Information: Baltic Sea Physics Analysis and Forecast, Marine Data Store (MDS), CMEMS [data set], <https://doi.org/10.48670/moi-00010>, 2024.
- Conte, D. and Lionello, P.: Characteristics of large positive and negative surges in the Mediterranean Sea and their attenuation in future climate scenarios, *Global Planet. Change*, 111, 159–173, <https://doi.org/10.1016/j.gloplacha.2013.09.006>, 2013.
- Dong, Z., Hu, H., Liu, H., Baiyin, B., Mu, X., Wen, J., Liu, D., Chen, L., Ming, G., Chen, X., and Li, X.: Superior performance of hybrid model in ungauged basins for real-time hourly water level forecasting – A case study on the Lancang-Mekong mainstream, *J. Hydrol.*, 633, 130941, <https://doi.org/10.1016/j.jhydrol.2024.130941>, 2024.
- ECMWF: Ensemble Prediction System (EPS) – 50-member global ensemble forecasts, retrieved via MARS (Meteorological Archival and Retrieval System), <https://www.ecmwf.int/en/forecasts/datasets> (last access: 24 April 2024), 2024.
- Ekman, M.: The changing level of the Baltic Sea during 300 years: a clue to understanding the Earth, <https://www.historicalgeophysics.ax/downloads/the-changing-level-of-the-baltic-sea.pdf> (last access: 13 July 2025), 2009.
- Elken, J., Maljutenko, I., Lagemaa, P., and Verjovkina, S.: Mere operatiivmudelisüsteemi NEMO kasutuselevõtt ja töölerakendamise mereala operatiivprognooside parandamiseks, *Tech. Rep. 82*, TTÜ Meresüsteemide Inst., https://keskkonnaportaal.ee/sites/default/files/andmekataloog/lisakirjeldus/NEMO_II_aruanne2021_v2.pdf (last access: 10 July 2025), 2021.
- Elken, J., Barzandeh, A., Maljutenko, I., and Rikka, S.: Reconstruction of Baltic gridded sea levels from tide gauge and altimetry observations using spatiotemporal statistics from reanalysis, Re-

- mote Sens.-Basel, 16, 2702, <https://doi.org/10.3390/rs16152702>, 2024.
- Estonian Environment Agency: Time series of hydrological monitoring data in JSON format, Estonian Environment Agency [data set], <https://keskkonnaportaal.ee/et/avaandmed/hydroloogilise-seire-andmestik> (last access: 13 July 2025), 2024.
- Ganaie, M., Hu, M., Malik, A., Tanveer, M., and Suganthan, P.: Ensemble deep learning: a review, *Eng. Appl. Artif. Intel.*, 115, 105151, <https://doi.org/10.1016/j.engappai.2022.105151>, 2022.
- Gröger, M., Arneborg, L., Dieterich, C., Höglund, A., and Meier, H. E. M.: Summer hydrographic changes in the Baltic Sea, Kattegat and Skagerrak projected in an ensemble of climate scenarios downscaled with a coupled regional ocean-sea ice-atmosphere model, *Clim. Dynam.*, 53, 5945–5966, <https://doi.org/10.1007/s00382-019-04908-9>, 2019.
- Hamlington, B. D., Gardner, A. S., Ivins, E., Lenaerts, J. T., Reager, J., Trossman, D. S., Zaron, E. D., Adhikari, S., Arendt, A., Aschwanden, A., Beckley, B. D., Bekaert, D. P. S., Blewitt, G., Caron, L., Chambers, D. P., Chandanpurkar, H. A., Christianson, K., Csatho, B., Cullather, R. I., DeConto, R. M., Fasullo, J. T., Frederikse, T., Freymueller, J. T., Gilford, D. M., Giroto, M., Hammond, W. C., Hock, R., Holschuh, N., Kopp, R. E., Landerer, F., Larour, E., Menemenlis, D., Merrifield, M., Mitrovica, J. X., Nerem, R. S., Nias, I. J., Nieves, V., Nowicki, S., Pangaluru, K., Picuch, C. G., Ray, R. D., Rounce, D. R., Schlegel, N.-J., Seroussi, H., Shirzaei, M., Sweet, W. V., Velicogna, I., Vinogradova, N., Wahl, T., Wiese, D. N., and Willis, M. J.: Understanding of contemporary regional sea-level change and the implications for the future, *Rev. Geophys.*, 58, e2019RG000672, <https://doi.org/10.1029/2019RG000672>, 2020.
- Hieronymus, M. and Hieronymus, F.: A novel machine learning based bias correction method and its application to sea level in an ensemble of downscaled climate projections, *Tellus A*, 75, 129–144, <https://doi.org/10.16993/tellusa.3216>, 2023.
- Hünicke, B. and Zorita, E.: Statistical analysis of the acceleration of Baltic mean sea-level rise, 1900–2012, *Front. Mar. Sci.*, 3, 125, <https://doi.org/10.3389/fmars.2016.00125>, 2016.
- Hünicke, B., Zorita, E., Soomere, T., Madsen, K., Johansson, M., and Suursaar, U.: Recent change – sea level and wind waves, in: *Second Assess. Clim. Chang. Balt. Sea Basin*, Springer, https://doi.org/10.1007/978-3-319-16006-1_9, 155–185, 2015.
- Ishida, K., Tsujimoto, G., Ercan, A., Tu, T., Kiyama, M., and Amagasaki, M.: Hourly-scale coastal sea level modeling in a changing climate using long short-term memory neural network, *Sci. Total Environ.*, 720, 137613, <https://doi.org/10.1016/j.scitotenv.2020.137613>, 2020.
- Jahanmard, V., Hordoir, R., Delpeche-Ellmann, N., and Ellmann, A.: Quantification of hydrodynamic model sea level bias utilizing deep learning and synergistic integration of data sources, *Ocean Model.*, 186, 102286, <https://doi.org/10.1016/j.ocemod.2023.102286>, 2023.
- Jandt-Scheelke, S., Panteleit, T., Verjovkina, S., Lagemaa, P., Spruch, L., and Morrison, H.: Quality Information Document: Baltic Sea Physical Analysis and Forecasting Product (BALTICSEA_ANALYSIS_FORECAST_PHY_003_006), cMEMS product quality coordination team, <https://catalogue.marine.copernicus.eu/documents/QUID/CMEMS-BAL-QUID-003-006.pdf> (last access: 10 July 2025), 2023.
- Jensen, C., Mahavadi, T., Schade, N. H., Hache, I., and Kruschke, T.: Negative storm surges in the Elbe estuary – large-scale meteorological conditions and future climate change, *Atmosphere-Basel*, 13, 1634, <https://doi.org/10.3390/atmos13101634>, 2022.
- Jevrejeva, S., Moore, J., and Grinsted, A.: Influence of the Arctic Oscillation and El Niño Southern Oscillation (ENSO) on ice conditions in the Baltic Sea: the wavelet approach, *J. Geophys. Res.-Atmos.*, 108, 4677, <https://doi.org/10.1029/2003JD003417>, 2003.
- Johansson, M., Kahma, K., Boman, H., and Launiainen, J.: Scenarios for sea level on the Finnish coast, *Boreal Environ. Res.*, 9, 153–166, 2004.
- Jönsson, B., Döös, K., Nycander, J., and Lundberg, P.: Standing waves in the Gulf of Finland and their relationship to the basin-wide Baltic seiches, *J. Geophys. Res.-Oceans*, 113, C03004, <https://doi.org/10.1029/2006JC003862>, 2008.
- Kärnä, T., Ljungemyr, P., Falahat, S., Ringgaard, I., Axell, L., Korabel, V., Murawski, J., Maljutenko, I., Lindenthal, A., Jandt-Scheelke, S., Verjovkina, S., Lorkowski, I., Lagemaa, P., She, J., Tuomi, L., Nord, A., and Huess, V.: Nemo-Nordic 2.0: operational marine forecast model for the Baltic Sea, *Geosci. Model Dev.*, 14, 5731–5749, <https://doi.org/10.5194/gmd-14-5731-2021>, 2021.
- Khojasteh, D., Glamore, W., Heimhuber, V., and Felder, S.: Sea level rise impacts on estuarine dynamics: a review, *Sci. Total Environ.*, 780, 146470, <https://doi.org/10.1016/j.scitotenv.2021.146470>, 2021.
- Kont, A., Jaagus, J., Aunap, R., Ratas, U., and Ravis, R.: Implications of sea-level rise for Estonia, *J. Coast. Res.*, 24, 423–431, <https://doi.org/10.2112/07A-0015.1>, 2008.
- Kulikov, E. and Medvedev, I.: Variability of the Baltic Sea level and floods in the Gulf of Finland, *Oceanology*, 53, 145–151, <https://doi.org/10.1134/S0001437013020094>, 2013.
- Leutbecher, M. and Palmer, T.: Ensemble forecasting, ECMWF, <https://doi.org/10.21957/c0hq4yg78>, 2007.
- Liu, Y. and Fu, W.: Assimilating high-resolution sea surface temperature data improves the ocean forecast potential in the Baltic Sea, *Ocean Sci.*, 14, 525–541, <https://doi.org/10.5194/os-14-525-2018>, 2018.
- Lou, R., Lv, Z., Dang, S., Su, T., and Li, X.: Application of machine learning in ocean data, *Multimedia Syst.*, 29, 1815–1824, <https://doi.org/10.1007/s00530-020-00733-x>, 2023.
- Madec, G., Bourdallé-Badie, R., Bouttier, P.-A., Bricaud, C., Bruciferri, D., Calvert, D., Chanut, J., Clementi, E., Coward, A., and Delrosso, D.: NEMO ocean engine, https://epic.awi.de/id/eprint/39698/1/NEMO_book_v6039.pdf (last access: 10 July 2025), 2017.
- Maljutenko, I., Elken, J., Lagemaa, P., and Verjovkina, S.: Mere operatiivmudelisüsteemi NEMO kasutuselevõtt ja töölerakendamine mereala operatiivprognooside parandamiseks, *Tech. rep.*, TTÜ Meresüsteemide Inst., https://keskkonnaportaal.ee/sites/default/files/andmekataloog/lisakirjeldus/NEMOaruanne2022_IIIetapp_puhas.pdf (last access: 13 July 2025), 2022.
- Mentaschi, L., Besio, G., Cassola, F., and Mazzino, A.: Problems in RMSE-based wave model validations, *Ocean Model.*, 72, 53–58, <https://doi.org/10.1016/j.ocemod.2013.08.003>, 2013.

- Mentaschi, L., Vousdoukas, M. I., García-Sánchez, G., Fernández-Montblanc, T., Roland, A., Voukouvalas, E., Federico, I., Abdolali, A., Zhang, Y. J., and Feyen, L.: A global unstructured, coupled, high-resolution hindcast of waves and storm surge, *Front. Mar. Sci.*, 10, 1233679, <https://doi.org/10.3389/fmars.2023.1233679>, 2023.
- Metzner, M., Gade, M., Hennings, I., and Rabinovich, A. B.: The observation of seiches in the Baltic Sea using a multi data set of water levels, *J. Marine Syst.*, 24, 67–84, [https://doi.org/10.1016/S0924-7963\(99\)00079-2](https://doi.org/10.1016/S0924-7963(99)00079-2), 2000.
- Miles, E., Spillman, C., Church, J., and McIntosh, P.: Seasonal prediction of global sea level anomalies using an ocean–atmosphere dynamical model, *Clim. Dynam.*, 43, 2131–2145, <https://doi.org/10.1007/s00382-013-2039-7>, 2014.
- Owens, R. and Hewson, T.: ECMWF Forecast User Guide, Tech. rep., Reading, <https://doi.org/10.21957/m1cs7h>, 2018.
- Pärt, S., Björkqvist, J.-V., Alari, V., Maljutenko, I., and Uiboupin, R.: An ocean–wave–trajectory forecasting system for the eastern Baltic Sea: validation against drifting buoys and implementation for oil spill modeling, *Mar. Pollut. Bull.*, 195, 115497, <https://doi.org/10.1016/j.marpolbul.2023.115497>, 2023.
- Ponte, R. M., Carson, M., Cirano, M., Domingues, C. M., Jevrejeva, S., Marcos, M., Mitchum, G., Van De Wal, R., Woodworth, P. L., Ablain, M., Arduin, F., Ballu, V., Becker, M., Benveniste, J., Birol, F., Bradshaw, E., Cazenave, A., De Mey-Frémaux, P., Durand, F., Ezer, T., Fu, L.-L., Fukumori, I., Gordon, K., Gravelle, M., Griffies, S. M., Han, W., Hibbert, A., Hughes, C. W., Idier, D., Kourafalou, V. H., Little, C. M., Matthews, A., Melet, A., Merrifield, M., Meyssignac, B., Minobe, S., Penduff, T., Picot, N., Piecuch, C., Ray, R. D., Rickards, L., Santamaría-Gómez, A., Stammer, D., Staneva, J., Testut, L., Thompson, K., Thompson, P., Vignudelli, S., Williams, J., Williams, S. D. P., Wöppelmann, G., Zanna, L., and Zhang, X.: Towards comprehensive observing and modeling systems for monitoring and predicting regional to coastal sea level, *Frontiers in Marine Science*, 6, 437, <https://doi.org/10.3389/fmars.2019.00437>, 2019.
- Raissi, M., Perdikaris, P., and Karniadakis, G.: Physics-informed neural networks: a deep learning framework for solving forward and inverse problems involving nonlinear partial differential equations, *J. Comput. Phys.*, 378, 686–707, <https://doi.org/10.1016/j.jcp.2018.10.045>, 2019.
- Rajabi-Kiasari, S., Delpeche-Ellmann, N., and Ellmann, A.: Forecasting of absolute dynamic topography using deep learning algorithm with application to the Baltic Sea, *Comput. Geosci.*, 178, 105406, <https://doi.org/10.1016/j.cageo.2023.105406>, 2023.
- Rus, M., Fettich, A., Kristan, M., and Ličer, M.: HIDRA2 – Deep-learning ensemble sea level and storm tide forecasting in the presence of seiches, Zenodo [code], <https://doi.org/10.5281/zenodo.7307365>, 2022.
- Rus, M., Fettich, A., Kristan, M., and Ličer, M.: HIDRA2: deep-learning ensemble sea level and storm tide forecasting in the presence of seiches – the case of the northern Adriatic, *Geosci. Model Dev.*, 16, 271–288, <https://doi.org/10.5194/gmd-16-271-2023>, 2023.
- Rus, M., Mihanović, H., Ličer, M., and Kristan, M.: HIDRA3: a deep-learning model for multipoint ensemble sea level forecasting in the presence of tide gauge sensor failures, *Geosci. Model Dev.*, 18, 605–620, <https://doi.org/10.5194/gmd-18-605-2025>, 2025.
- Rutgersson, A., Kjellström, E., Haapala, J., Stendel, M., Danilovich, I., Drews, M., Jylhä, K., Kujala, P., Larsén, X. G., Halsnæs, K., Lehtonen, I., Luomaranta, A., Nilsson, E., Olsson, T., Särkkä, J., Tuomi, L., and Wasmund, N.: Natural hazards and extreme events in the Baltic Sea region, *Earth Syst. Dynam.*, 13, 251–301, <https://doi.org/10.5194/esd-13-251-2022>, 2022.
- Samuelsson, M. and Stigebrandt, A.: Main characteristics of the long-term sea level variability in the Baltic sea, *Tellus A*, 48, 672–683, <https://doi.org/10.1034/j.1600-0870.1996.t014-00006.x>, 1996.
- Scotto, M., Barbosa, S. M., and Alonso, A. M.: Model-based clustering of Baltic sea-level, *Appl. Ocean Res.*, 31, 4–11, <https://doi.org/10.1016/j.apor.2009.03.001>, 2009.
- Shahabi, A. and Tahvildari, N.: A deep-learning model for rapid spatiotemporal prediction of coastal water levels, *Coast. Eng.*, 190, 104504, <https://doi.org/10.1016/j.coastaleng.2024.104504>, 2024.
- Sonnewald, M., Lguensat, R., Jones, D. C., Dueben, P. D., Brajard, J., and Balaji, V.: Bridging observations, theory and numerical simulation of the ocean using machine learning, *Environ. Res. Lett.*, 16, 073008, <https://doi.org/10.1088/1748-9326/ac0eb0>, 2021.
- Suursaar, Ü., Kullas, T., and Otsmann, M.: A model study of the sea level variations in the Gulf of Riga and the Väinameri Sea, *Cont. Shelf Res.*, 22, 2001–2019, [https://doi.org/10.1016/S0278-4343\(02\)00046-8](https://doi.org/10.1016/S0278-4343(02)00046-8), 2002.
- Tanjajura, C. A. S., Lima, L. N., and Belyaev, K. P.: Assimilation of satellite surface-height anomalies data into a Hybrid Coordinate Ocean Model (HYCOM) over the Atlantic Ocean, *Oceanology*, 55, 667–678, <https://doi.org/10.1134/S0001437015050161>, 2015.
- Taylor, K. E.: Summarizing multiple aspects of model performance in a single diagram, *J. Geophys. Res.-Atmos.*, 106, 7183–7192, <https://doi.org/10.1029/2000JD900719>, 2001.
- Weisse, R., Dailidienė, I., Hünicke, B., Kahma, K., Madsen, K., Omstedt, A., Parnell, K., Schöne, T., Soomere, T., Zhang, W., and Zorita, E.: Sea level dynamics and coastal erosion in the Baltic Sea region, *Earth Syst. Dynam.*, 12, 871–898, <https://doi.org/10.5194/esd-12-871-2021>, 2021.
- Wolski, T. and Wiśniewski, B.: Characteristics and long-term variability of occurrences of Storm surges in the Baltic Sea, *Atmosphere-Basel*, 12, 1679, <https://doi.org/10.3390/atmos12121679>, 2021.
- Wolski, T., Wiśniewski, B., Giza, A., Kowalewska-Kalkowska, H., Boman, H., Grabbi-Kaiv, S., Hammarklint, T., Holfort, J., and Žydrune Lydeikaitė: Extreme sea levels at selected stations on the Baltic Sea coast, *Oceanologia*, 56, 259–290, <https://doi.org/10.5697/oc.56-2.259>, 2014.
- Zhang, Y., Liu, J., and Shen, W.: A review of ensemble learning algorithms used in remote sensing applications, *Appl. Sci.-Basel*, 12, 8654, <https://doi.org/10.3390/app12178654>, 2022.
- Zhu, Z., Wang, Z., Dong, C., Yu, M., Xie, H., Cao, X., Han, L., and Qi, J.: Physics informed neural network modelling for storm surge forecasting – A case study in the Bohai Sea, China, *Coast. Eng.*, 197, 104686, <https://doi.org/10.1016/j.coastaleng.2024.104686>, 2025.